CHAPTER VI
EFFECT OF DIELECTRIC CONSTANT AND ELECTRIC FIELD STRENGTH ON DIELECTROPHORESIS FORCE OF ACRYLIC ELASTOMERS AND STYRENE COPOLYMERS

Abstract

The effects of dielectric constant and electric field strength on the deflection angle and the dielectrophoresis force of acrylic elastomers and styrene copolymers were investigated. The dielectrophoresis forces of six elastomers were determined in a vertical cantilever fixture by measuring the deflection distance under various electric field strengths. The forces were calculated from the non-linear deflection theory of the cantilever. As an electric field is applied, five elastomers, with the exception of SAR, deflect towards the anode side of the electrodes. For these elastomers, internal dipole moments are generated under electric field leading to the attractive force between the elastomers and the anode. SAR contains metal impurities (Cu and Zn) determined by EDX. Their presence introduces a repulsive force between the Cu^{2+} and Zn^{2+} ions and the aniodic electrode, leading to the bending towards the neutral electrode. The dielectrophoresis forces of the six elastomers generally increase with increasing electric field strength, and increase monotonically with the dielectric constants. AR71 ($\varepsilon' = 6.33$) has the lowest electrical yield point (75 V/mm) but it generates the highest force. On the other hand, SIS ($\varepsilon' = 2.74$) has the highest electrical yield point (400 V/mm) and it generates the lowest force.

Keyword: dielectric properties, elastomers, dielectrophoresis force, block copolymers, electromechanical responses

Introduction

Electroactive polymers are prospective materials for many applications such as actuation in MEMS devices and artificial muscles. These types of polymers are materials that can convert electrical energy into a shape change [1]. Efficient actuators require low driving energy, light weight, low cost, and ease of processing. Dielectric elastomers are suitable because they have many advantages, such as a light weight, a high degree of mechanical response, and a fast response time. There has been much interest recently in using dielectric elastomers as electroactive materials [1]: acrylic elastomers [2], silicone elastomers [3–5], and polyurethane [6, 7].

Zrinyi et al. [4] studied the bending of poly(dimethyl siloxane) gel containing finely dispersed TiO_2 particles. They studied the bending of polymers between two electrodes of two geometries: the first geometry employed dielectric polymers between two compliant electrodes; and the second geometry placed a polymer gel between a pair of fixed electrodes [4].

Pelrine et al. (1998 [1] and 2002 [8]) studied the behavior of various types of dielectric elastomers by coating the specimens with two compliant electrodes under an applied electric field. They determined the % strain changes and calculated the electromechanical efficiency of the elastomers, and concluded that the dielectric elastomers having high dielectric constants generated high degrees of electromechanical response. The resultant effective pressure can be expressed as:

$$p = \varepsilon\varepsilon_0 E^2 \quad , \tag{1}$$

where p is the effective pressure, ε is the dielectric permittivity of the material, ε_0 is the dielectric constant of free space (8.85 pF/m), and E is the electric field strength (V/m) [1].

Diaconu et al. [9] investigated the electromechanical strain? responses of a polyurethane elastomer-based polyester. They found that the deformation of elastomers under applied electric field strength came from 2 effects. The first is Maxwell stress and the second is electrostriction. The Maxwell stress is the force that is generated by the attractive force between unlike charges on the top and bottom electrode surfaces under applied electric field [8]. On the other hand, electrostriction

is the direct coupling between an electric polarization and the mechanical response of the materials [9]. The ratio between Maxwell stress and electrostriction on the electromechanical response depends on the chemical composition, processing conditions of the sample, and thermal and mechanical treatment of the materials [9]. The strain response from the electrostriction can be expressed as:

$$e = -Q\varepsilon_0^2(\varepsilon - 1)^2 E^2 \ , \qquad (2)$$

where e is the strain, Q is the electrostriction coefficient, ε is the dielectric permittivity of the material, ε_0 is the dielectric constant of free space (8.85 pF/m), and E is the electric field strength (V/m) [9]. Using Hooke's law:

$$\delta = -Q\varepsilon_0^2(\varepsilon - 1)^2 E^2 Y \ , \qquad (3)$$

where δ is the stress.From equations 1 and 3, it is expected that the stress should vary linearly with the dielectric constant and the square of the electric field strength.

Watanabe et al. [10] studied the electromechanical responses of pure polyurethane with compliant electrodes. The responses were due to the difference in charge densities between the anode and the cathode. Hiamtup et al. [11] studied the dielectrophoresis force of polymer blends of polyaniline and polydimethylsiloxane with fixed copper electrodes. The dielectrophoresis force increases with increasing electric field strength but decreases with increasing polyaniline concentration. Niamlang et al. [12, 13] investigated the dielectrophoresis force of pure polydimethylsiloxane and polymer blends of polydimethylsiloxane and poly(p-phenylenevinylene). The conductive polymer particles enhanced the dielectrophoresis force.

In our work, we investigate the electromechanical responses of acrylic elastomers (AR70, AR71, and AR72), styrene-acrylic copolymers (SAR), and tri–block copolymers (SIS and SBR) in terms of the deflection angle and the dielectrophoresis force. In particular, the dielectric constants will be shown to be well correlated with the deflection angle and the dielectrophoresis force. We focus on the effect of electric field strength on the deflected distance and direction, and on the dielectrophoresis force at room temperature. In addition, we calculated and compared the electromechanical efficiency, the power density, the energy density, the force density, the power consumption, and the efficiency for use as artificial muscles.

Experimental

Materials

Acrylic elastomers Nipol AR71 (T_g = 258 K) and AR72 (T_g = 245 K) were provided by Nippon Zeon Polymix Advance Co., Ltd. The acrylic elastomer AR7018 (AR70), Styrene-Butadiene rubber latex (UCAR DL849, T_g = 312 K), and Styrene-Acrylic-copolymer latex (UCAR DA27, T_g = 297 K) were provided by Dow Chemical Co., Ltd. A Styrene-isoprene-styrene triblock copolymer (SIS Kraton D1112P) was obtained from Shell of Thailand Co., Ltd. The silicone oil, poly(dimethylsiloxane) 200® fluid, was supplied by Dow Corning Corp. The oil had a kinematic viscosity of 100 cSt, and was used as the medium in the deflection experiments.

Preparation of Specimens

All elastomer specimens were fabricated through solution casting. AR70, SAR, and SBR specimens were formed by water evaporation; the SIS D1112P, AR71, and AR72 specimens were dissolved in toluene at 30 % vol/vol. The solutions were cast onto a mold and the solvent was eliminated under a vacuum atmosphere at 300 K for 72 hours. Each sample was cut into a thin ribbon (length $\approx$ 23 mm, width $\approx$ 2.5 mm, and thickness $\approx$ 0.5 mm). The specimens were immersed in the silicone oil 200® fluid overnight before testing.

Characterization and Testing

Dielectric constants were measured by an LCR meter (HP, model 4284A) connected to a rheometer (Rheometric Scientific, ARES) fitted with a 25 mm parallel plate fixture. The thickness of the specimens was typically 1 mm and the diameter was about 25 mm. Before each measurement, the top and bottom sides of the specimens were coated with a silver adhesive to improve the electrical contact between the specimens and the electrodes. (The dielectric constant at the frequency equal 20 Hz will be referred to as the dielectric constant of the materials.)

The six elastomers were characterized by an FT-IR spectrometer in order to identify their functional groups. The FT-IR spectrometer (Thermo Nicolet, Nexus 670) was operated in absorption mode with 32 scans at resolution of $\pm$ 4 cm^{-1},

covering a wavenumber range between 400 and 4.000 cm^{-1}, using a deuterated triglycine sulfate detector. The specimens were prepared as thin films (thickness ≈ 0.5 mm).

The percentages of elements (Cu, Zn, Fe, Cl, Na, C, and O) in the elastomers were characterized and determined by an EDX (Energy Dispersive X-Ray Fluorescence Spectrometer, OXFORD Pentafet, model 6111); it was also connected to a scanning electron microscope (JEOL, model JSM-5200).

The dielectrophoresis forces were determined by measuring the deflection distances of the elastomers in the vertical cantilever fixture under electric field. (The experimental setup is shown in Figure 1.) The specimens were vertically immersed in the silicone oil (viscosity = 100 cSt) between parallel copper electrode plates (40 mm long, 30 mm width, and 1 mm thick). The gap between the pair of electrodes was 30 mm. A DC voltage was applied with a DC power supply (Goldsun, GPS 3003B) connected to a high voltage power supply (Gamma High Voltage, model UC5-30P and UC5-30N) which can deliver an electric field up to 25 kV. The output voltage from the high voltage power supply was calibrated using a Fluke 40 kV High Voltage Probe. We used a CCD video camera to record the movement during the experiment. Still pictures were captured from the video and the deflection distances in x (d) and y axes (l) at the ends of the specimen were determined by using Scion Image software (version 4.0.3). The electric field strength was varied between 0–600 V/mm at room temperature, 300 ± 1 K. Both the voltage and the current were monitored. We calculated the resisting elastic force of the specimens under electric field using the non-linear deflection theory of a cantilever [12-16], which can be calculated from the standard curve between $\frac{F_e l_0^2}{EI}$ and $\frac{d}{l_0}$ (l_0 = initial length of specimens) [15].

where F_e is the elastic force, d is the deflection distance in the horizontal axis, l is the deflection distance in the vertical axis, E is the Young's modulus —which is equal to $2G(1+\nu)$, where G is the shear storage modulus taken to be $G'(\omega = 1$ rad/s) at various electric field strengths and, ν is the Poisson's ratio (0.5 for an incompressible sample)— and I is the moment of inertia $\frac{1}{12} t^3 w$, where t is the thickness of the film

and w is the width of the film. The dielectrophoresis force can be calculated from the static horizontal force balance consisting of the elastic force and the corrective gravity force term ($mg\sin\theta$):

$$F_d = F_e + mg\sin\theta \ , \qquad (4)$$

where g = 9.8 m.s^{-2}, m = mass of the specimen, and θ is the deflection angle.

To investigate the materials as potential actuators, the energy density, force density, mechanical power, power density, the electromechanical efficiency of the elastomers are important factors for comparison. These factors were calculated using equations 4 to 9, respectively [7-16]:

$$\text{Energy density} = \frac{1}{2}E\theta^2 \ \text{(J)} \ , \qquad (5)$$

$$\text{Force density} = \frac{F_d}{volume} \ \text{(N.cm}^{-3}\text{)} \ , \qquad (6)$$

$$\text{Mechanical power} = \frac{1}{4}F_d\frac{d}{\tau_i} \ \text{(W)} \ , \qquad (7)$$

$$\text{Power or work density} = \frac{\text{mechanical power}}{\text{volume}} \ \text{(W.cm}^{-3}\text{)} \ , \qquad (8)$$

$$\text{Electromechanical coupling efficiency} = \frac{\text{mechanical power}}{\text{power consumption}} \text{x}100\% = \frac{(1/4)*F_d*d}{\text{induction time}*\text{power consumption}} \text{x}100\% \qquad (9)$$

where τ_i is the induction time.

Results and Discussion

Dielectric constant of the elastomers

From the previous work [17], the dielectric constants of AR70, AR71, AR72, SAR, SIS D1112P, and SBR, obtained at T = 300 K at a frequency of 20 Hz, are 6.21, 6.33, 4.14, 3.95, 2.74, and 2.87, respectively [17]. The dielectric constants decrease slightly with increasing frequency due to the decrease of the interfacial polarization. The dependence of the dielectric constant on frequency can be expressed as [18]:

$$\varepsilon' = \varepsilon_\infty + \frac{(\varepsilon_s - \varepsilon_\infty)}{1 + \omega^2 \tau^2} \quad , \tag{10}$$

where ε' is the dielectric constant, ε_∞ is dielectric constant at infinitely high frequency, ε_s is the dielectric constant at low frequency, ω is frequency, and τ is the relaxation time [18].

Effect of electric field strength and dielectric constants on deflection angle

The effects of electric field strength and dielectric constants on the deflection angle were investigated under the electric field strengths between 0 and 600 V/mm within the temperature of 300 ± 1 K. (Still pictures of our experiments are shown in Figures 2(a)–2(f)). Initially, all of specimens are straight at the center of the testing fixture without electric field. After applying an electric field, the specimens start to deflect towards one of the electrodes. All materials deflect towards the anode side, with the exception of SAR, which deflects toward the neutral side. The electrical yield strength—the electric field strength required for the materials to start to deflect—of AR70, AR71, AR72, SAR, SIS, and SBR are 225, 75, 75, 250, 400, and 375 V/mm, respectively. These suggest that AR71 and AR72 require the lowest electrical energy to respond. The induction time— the period of time that the elastomers required for deflected to the maximum distance after applied electric field—of AR70, AR71, AR72, SAR, SIS, and SBR at E = 600 V/mm are 7, 3, 5, 9, 10, and 15 sec, respectively. The recovery time— the period of time that the elastomers required for deflected to the starter point after turn off the electric field—of AR70, AR71, AR72, SAR, SIS, and SBR at E = 600 V/mm are 25, 20, 18, 20, 7, and 8 sec, respectively. Figure 3(a) shows the deflection angles of the elastomers versus electric field strength. The deflection angles generally become larger with

increasing electric field strength. At E = 600 V/mm, AR71 shows the highest deflection angle, at 70.4 degrees, whereas SBR shows the lowest angle of only 8.6 degree. Figure 3(b) shows the correlation between the deflection angle and the dielectric constants of the elastomers investigated. From Figure 3(b), we can see that the AR71 has the highest dielectric constant and responds with the highest deflection angle, whereas SIS D1112P and SBR have the lowest dielectric constants and corresponding deflection angles. Figures 3 (a) and (b) thus show the results consistent with the electrostriction theory [9]. As the electric field is applied, the dipole moments of molecules are generated. The functional and/or polar groups on the polymer chains are polarized as the result of electric field. As the electric field strength increases, this leads to a further increase in the internal dipole moments. This leads to the increases in the degree of interaction with the electrodes, the deflection angle, and the corresponding mechanical strains.

Metz et al. [19] investigated the bending behavior of polymer blends of PVDF and PPy. They found that the bending angle and the bending moment increased linearly with increasing electric field strength. Hirai et al. [20] studied the effect of plasticizer type on the deflection angle of poly(vinyl chloride) gels. They reported that the dielectric constant of the plasticizers in poly(vinyl chloride) gels was not related with the deflection angle. The chemical structure of the plasticizers, however, appears to be an important factor affecting the electromechanical response of the poly(vinyl chloride) gels [20].

Effect of electric field strength and dielectric constants on the dielectrophoresis force

The elastic force and the dielectrophoresis force of the elastomers were calculated from the deflection distance using the non-linear deflection theories of a cantilever [14, 15]. The effect of electric field strength on the dielectrophoresis force is shown in Figure 4(a). The dielectrophoresis forces of our materials are measurable at their electrical yield strengths. The forces increase nonlinearly with increasing electric field strength due to the increase in the internal dipole moments and the electric polarization of the materials. The forces become saturated at high electric

field strength. The relationship between the electrical polarization and electric field strength can be expressed as [18]:

$$P = (\varepsilon - 1)\varepsilon_0 E \quad , \quad (11)$$

where P is the electrical polarization, ε is the dielectric constant of materials, ε_0 is the dielectric constant of vacuum, and E is the electric field strength, d is the thickness [18].

At the electric field strength of to 600 V/mm, the acrylic elastomers AR71 generates the highest dielectrophoresis force (389 μN), and SIS D1112P generates the lowest force (67 μN). Figure 4(b) shows a correlation between the dielectrophoresis force and the dielectric constant of the elastomers; the dielectrophoresis force depends nonlinearly with the dielectric constant and it becomes saturated at high dielectric constant.

Watanabe et al. [21] reported that as the electric field was turned on, the charges were injected from one side of the electrode to the opposite side [21]. The charges can be accumulated in the materials as the dipole polarization and the space charges. Under electric field, the materials become polarized, as the polarizability of dielectric materials depends on the dielectric constant. The highly dielectric materials can be polarized easier and stronger internal dipole moments generated. Based on the electrostriction theory, the elastomers that have higher dielectric constants are expected to generate higher resultant forces at the same applied voltage [8, 21]. Carpi et al. [22] reported that the strain responses under applied electric field of the dielectric elastomers strongly depend on the dielectric permittivity of polymers, as well as on the modulus of elasticity [22].

Characterization of the elastomers by FT-IR

As reported in the previous part, all of the elastomers, except SAR, deflect towards the anode side. To determine the cause of this occurrence, the chemical compositions and structures of our elastomers were determined. FT-IR spectra of the acrylic elastomers (AR70, AR71, and AR72) were taken to identify the characteristic absorption peaks. The characteristic peaks of the acrylic elastomers are at 1728 cm^{-1}, 1410 cm^{-1}, 1390 cm^{-1}, and 1150 cm^{-1}. These peaks can be assigned to the C=O

stretching on the ester group [23], the $CO-CH_2$ ester group [23]. the methyl or ethyl group [23], and the C-O stretching on the ester group [23], respectively.

The characteristic peaks of the styrene-acrylic copolymer (SAR) are at 1715 cm^{-1}, 1500–1430 cm^{-1}, 1200–1100 cm^{-1}, 751 cm^{-1} and 649 cm^{-1}. These peaks can be assigned to the the C=O stretching on the ester group [24], the $CO-CH_2$ ester group [23], C=C stretching on benzene ring [24]; the C-O stretching on the ester group [24], and the C-H stretching on the mono-substituted benzene ring [23], respectively

The FT-IR spectra of the styrene-isoprene-styrene triblock copolymer (SIS) shows the characteristic peaks at 1450 cm^{-1}, 1380 cm^{-1}, 1200–1100 cm^{-1}, 889 cm^{-1}, and 760 cm^{-1} and 698 cm^{-1}. These peaks can be assigned to the C=C vibrating on the benzene ring [24], the methyl or ethyl group [23], the C-O stretching on the ester group [23], the di-substituted of isoprene [23], and the C-H stretching on the mono-substituted benzene ring [23], respectively.

The FT-IR spectrum of the styrene-butadiene rubber (SBR) shows the characteristic peaks at 3300 cm^{-1}, 1620–1600 cm^{-1}, 1450 cm^{-1}, 1020 cm^{-1}, 966 cm^{-1}, and 760 cm^{-1} and 698 cm^{-1}. These peaks can be assigned to the mono-substituted butadiene [24], the C-C stretching on the mono-substituted benzene ring, the C=C vibrating on the benzene ring [23], the =CH-R stretching on the butadiene [23], the 1,2 tran C-H wagging of butadiene [23], and the C-H stretching on mono-substituted benzene ring [23], respectively.

In summary, the FTIR peaks of the materials investigated are consistent with those found previously; there is no anomalous peak present that can be observed.

The deflected direction of the elastomers

All the elastomers deflect towards the anode side, except SAR, which deflects towards the opposite side. From the FT-IR spectra, the origin of the opposite deflection cannot be identified. In the work by Watanabe et al [20, 21], they studied the effect of dopant types on the bending of doped polyurethanes. They found that the undoped polyurethane bent towards the cathode side. For the doped polyurethanes of various salts, the bending direction of polyurethane reversed depending on the type of the dopants used [21].

To investigate further the origin of the opposite deflection direction, we used the EDX (Energy Dispersive X-Ray Fluorescence Spectrometer) technique to

determine the percentages of elements in our elastomers. In the cases of the acrylic elastomer AR70, and styrene-isoprene-styrene triblock copolymer, the percentage of atomic Cu and Zn metals are equal to 0.02% and 0.00% for the AR70, and 0.02% and 0.03% for SIS, respectively. But for SAR, the percentage of atomic Cu and Zn metals are 0.15% and 0.30%, respectively.

In the case of the acrylic elastomers, the deflection direction depends on the internal dipole polarization of the functional groups on the polymer chains [19]. The chemical structures of the acrylic elastomers (AR70, AR71, and AR72) have many ester and the carbonyl groups on the polymer chains. These polar groups can be aggregated to form polar crystalline regions [25]. This region can be polarized and can store energy under the electric field, which leads to dimensional changes within the polymer [20]. In addition, the ester and carbonyl groups are electrophiles, which can pull electrons from carbon atoms. Under the electric field strength, the polarities of the groups become negative and generate the attractive force between unlike charges on the anode electrode and the acrylic elastomers leads to the bending towards the anode side (positive side). The mechanism is shown in Figures 5(b).

In the case of SIS and SBR, the chemical structures of the styrene-isoprene-styrene triblock copolymer (SIS) and the styrene-butadiene elastomers (SBR) consist of many phenyl groups on the polymer chains. Under the electric field, the phenyl groups can also pull electrons from the carbon atoms on the backbone. The polarities of the phenyl group become negative. This leads to the apparent deflection towards the anode (positive) side. The mechanism is shown in Figures 5(c).

But in the case of the styrene-acrylic elastomers (SAR), which deflects towards the neutral electrode, there is another mechanism. As indicated by the EDX results, small amounts of Cu and Zn in our styrene-acrylic elastomers (SAR) are present. Under electric field, Cu and Zn atoms can be ionized to become Cu^{2+} and Zn^{2+} [21]. That leads to the positive charges generated within the specimens. In addition the carbonyl and phenyl groups can be polarized to become negative. Apparently, the effect of the positive charges of the metal ions is stronger than the negative charges from the dipole polarization of the carbonyl groups and the phenyl groups. Therefore, the competing effects lead to the deflection of SAR towards the neutral electrode. The mechanism is shown in Figures 5(d). To confirm this

hypothesis, we repeated our experiments but we changed the electrical polarity of the electric field from positive to negative polarity using the Gamma High Voltage model UC5-30N. SIS and SAR were used as the test specimens. The results are shown in Figure 2(g) and 2(h). SAR deflects away from the neutral electrode side due to the attractive force between positive charges, Cu^{2+} and Zn^{2+}, within the SAR and the negative charges on the cathode. In the case of SIS, it bends towards the neutral side due to the repulsive force between the negative charges on the specimens and the cathode side. Thus, it has been shown that the polarity of the elastomers under applied electric field can be used control the deflected direction and the degree of bending, the latter being concentration dependent.

Watanabe et al. [21] showed that Cu and Zn metals can be ionized to Cu^{2+} and Zn^{2+} under applied electric field. Zrinyi et al. [4] studied the bending of poly(dimethyl siloxane) gel containing finely dispersed TiO_2 particles. Under applied electric field, TiO_2 emitted electrons. TiO_2 particles become positively charged and the whole domain of the PDMS/TiO_2 bent towards the cathode side [4]. Yun et al. [27] studied the electromechanical responses of electroactive cellulose under electric field. They found that the electroactive cellulose bent towards the anode side due to the migration of the water molecules [27]. Yamauchi et al. [28] investigated the bending of the Polypyrrole and Poly(2-acrylamide-2-methyl propane) blends. The results show that the gels bent towards the cathode side. This was caused by the attractive force between anions on the sulfonic acid group of the polymer chains and the negative charges on the cathode [28].

Electromechanical responses of dielectric elastomers

The electromechanical responses of the dielectric elastomers were calculated to determine the efficiency for use as artificial muscle. The results are shown in Table 1. Energy density represents the ability of work that can be achieved by materials [14, 25]. From Table 1, AR70 has the highest energy density (62,114 $J.m^{-3}$); whereas SIS has the lowest (1,428 $J.m^{-3}$). AR71 generates the highest (28,012 $N.m^{-3}$) and SIS generates the lowest (3,392 $N.m^{-3}$).

Della Santana et al. [26] studied the deflection of polypyrrole in a horizontal cantilever contained in an electrolyte. They found that the energy density of

polypyrrole is as high as 73,000 $J.m^{-3}$ [26]. When comparing with our AR70 which PPy provided higher energy density than our elastomers.

Shahinpoor [27] studied the bending of ionic polymeric-conductor composites. He found that his composites can generate the force density at 10.7-15.6 mN. [27].

Alici *et al.*, [28] reported that the actuators base on polymer composites between polypyrrole and polyvinylidine fluorine can provide the output force equal to 0.6 mN at E = 1 V [28]. Dai *et al.*, [29] studied the bending force under applied electric field of ionic network membrane based on blends of water soluble poly (vinyl alcohol) (PVA) and highly ionic conductive poly 2-acrylamido-2-methyl-1-propanesulfonic acid (PAMPS). The bending force of PVA/PAMPS blend is equal to 4.9 mN at E = 40 V/mm [29]. When comparing with our AR71 which gave the dielectrophoresis force at 0.412 mN.

In the case of power, or work density.AR71 has the highest work density (31.01 $W.m^{-3}$) whereas SIS has the lowest (0.102 $W.m^{-3}$). When comparing our systems with the conductive polymers such as PPy that studied by Madden [30]. Polypyrrole provided the power density at 70-100 KJ/m^3. Whereas the NiTi Shape Memory Alloys can generate the power density more than 1000 KJ/m^3 [30].

Mechanical power is the ability of an actuator to convert electrical energy to mechanical energy [31]. AR71 has the highest mechanical power (0.456 μW); whereas SIS has the lowest (0.004 μW). The electromechanical coupling efficiency indicates the efficiency of materials in converting electrical energy to mechanical energy. Electromechanical coupling efficiency is the ratio between the mechanical power and the electrical power consumption of materials, as shown in equation (9). We calculated the power consumption of our systems by measuring the electrical current during the experiments. In our work, the AR72 requires the highest power consumption (7.3 mW); whereas the SBR requires the lowest (0.53 mW). The electromechanical coupling efficiency of AR71 is the highest (0.013%), and SBR is the lowest (0.0004%). From Table 1, we may conclude that the dielectric constant of the elastomers is the main factor controlling the electromechanical responses.

Yun et al. [31] studied the mechanical power and the electromechanical coupling efficiency of electroactive celluloses. They reported that both parameters

depended on the thickness of the specimens. When the thickness was equal to 20, 30, and 40 μm, the mechanical powers of the electroactive cellulose specimens were 10, 580, and 3.1 μW, respectively. The power consumptions were about 12, 17.5, and 55 mW, respectively. The electromechanical coupling efficiency of electroactive celluloses were 0.08, 3.3, and 0.056%, respectively [31]. Kim et al. [32] studied the deflection of electroactive cellulose under applied electric field. They reported that the electrical yield strength of electroactive cellulose was equal to 50 V/mm and the elastic force of their specimens was equal to 0.45 mN.

When comparing the electroactive cellulose and our acrylic elastomers, the acrylic elastomers give lower mechanical power and electromechanical coupling efficiency than the electroactive cellulose. These results mainly come from the differences in thickness between our materials (≈ 0.5 mm) and the electroactive cellulose specimens (≈ 20-40 μm). Mazzoldi et al. [33] studied the bending of polymer blends of poly(vinyl alcohol) and carbon nanotubes. The results showed that the PVA and carbon nanotube blends bent under applied electric field, with a bending distance of 0.15 mm.

Although the acrylic elastomers can provided work density and mechanical force lower than pure conductive polymer {Ppy) [30, 34], electroactive cellulose [31, 32] and Shape Memory Alloys [30]. But the dielectric elastomers can be developing for intermittent tasks such as gross position control and in artificial muscle [30].

Conclusion

In our study, the deflection angle and the dielectrophoresis force of AR70, AR71, AR72, SAR, SIS D1112P, and SBR were investigated by examining the effects of the electric field strength and the dielectric constant. The deflection angle and the dielectrophoresis force of all elastomers increases with electric field, and becomes saturated at high electric field strength for AR71 and AR72. Both parameters increase nonlinearly with increasing dielectric constant. The materials with high dielectricity require low electrical energy to respond. The acrylic elastomers (AR70, AR71, and AR72), styrene-butadiene rubber (SBR), and styrene-isoprene-styrene triblock copolymer (SIS) deflect towards the anode side under

applied electric field due to the polarity of polar groups on the polymer chains [25]. On the other hand, the styrene-acrylic copolymer deflects towards the opposite side. This behavior results from the Cu and Zn metal ions residing within the SAR. The ions can be ionized to become positively charged (Cu^{2+} and Zn^{2+}) under applied electric field [21]. We also calculated the power density, energy density, force density, mechanical power, power consumption, and electromechanical coupling efficiency of the elastomers; all of these parameters depend critically on the dielectric constant of the elastomers.

Acknowledgements

The authors would like to acknowledge the financial support from the following: the Conductive and Electroactive Polymers Research Unit and KFAS, both from Chulalongkorn University; the Petroleum, Petrochemical, and Advanced Materials Consortium; the Royal Thai Government Budget (Fiscal Year 2551); and the Thailand Research Fund, BRG and PhD/0182/2548. The material supports from Shell in Thailand Co. Ltd., Nippon Zeon Polymix Advance Co. Ltd., and Dow Chemical Co. Ltd. are also gratefully acknowledged.

References

1 R. Kornbluh, R. Pelrine, Q. Pei, S. Chiba, J. Joseph, High-field deformation of elastomeric dielectrics for actuators, Mat. Sci. Eng. C 11 (2002) 89-100.

2 W. Ma, L.E. Cross, An experimental investigation of electromechanical response in a dielectric acrylic elastomer, Appl. Phy. A 78 (2004) 1201.

3 M. Wissler, E. Mazza, Modeling of a pre-strained circular actuator made of dielectric elastomers, Sensor Actuat. A-Phy. 120 (2005) 184-192.

4 J. Feher, G. Filipcsei, J. Szalma, M. Zrinyi, Bending deformation of neutral polymer gels induced by electric fields, Colloid. Surface. A 183 (2001) 505-515.

5 Z. Varga, G. Filipcsei, A. Szilagyi, M. Zrinyi, Electric and Magnetic Field-Structured Smart Composites, Macromol. Symp. 227 (2005) 123-134.

6 R. Palakodeti, M.R. Kessler, Influence of frequency and prestrain on the mechanical efficiency of dielectric electroactive polymer actuators, Mater. Lett. 60 (2006) 3437-3440.

7 Y. Jung, H. Park, N. Jo, H. Jeong, Fabrication and performance evaluation of diaphragm-type polymer actuators using segmented polyurethane according to chemical-hard-segment content, Sensor Actuat. A-Phy. 136 (2007) 367-373.

8 R.E. Pelrine, R.D. Kornbluh, J.D. Joseph, Electrostriction of polymer dielectrics with compliant electrodes as a means of actuation, Sensor Actuat. A-Phy. 64 (1998) 77-85.

9 I. Diaconu, D.O. Dorohoi, F. Topoliceanu, Electrostriction of a Polyurethane Elastomer-Based Polyester, IEEE Sensors J. 6 (2006) 876.

10 M. Watanabe, T. Hirai, Space charge distribution in bending-electrostrictive polyurethane films doped with salts, J. Polym. Sci. B. 42 (2004) 523-531.

11 P. Hiamtup, A. Sirivat, A.M. Jamieson, Electromechanical response of a soft and flexible actuator based on polyaniline particles embedded in a cross-linked poly(dimethyl siloxane) network, Mat. Sci. Eng. C 28 (2007) 1044-1051.

12. S. Niamlang, A. Sirivat, Electromechanical responses of a crosslinked polydimethylsiloxane, Macromol. Symp. 264 (2007)176-183.

13 S. Niamlang, A. Sirivat, Dielectrophoresis force and deflection of electroactive poly(p-phenylene vinylene)/polydimethylsiloxane blends, Smart. Mater. Struc. 17 (2008) art. no. 035036.

14 J. Kim, K. Kang, S. Yun, Blocked force measurement of electro-active paper actuator by micro-balance, Sensor Actuat. A-Phy. 133 (2007) 401-406.

15 S.P. Timoshenko, J.M. Gere: Mechanics of Materials, 3rd Edition, Chapman & Hall, New York, USA.

16 T.S. Smith, R.M. Seugling, Sensor and actuator considerations for precision, small machines, Precis. Eng. 30 (2006) 245-264.

17 R. Kunanuruksapong, A. Sirivat, Electrical properties and electromechanical responses of acrylic elastomers and styrene copolymers: effect of temperature, Appl. Phys. A.96 (2008) 313.

18 G.G. Raju. Dielectrics in Electric Fields, University of Windsor, Windsor. Ontario, Canada, 2003.

19 P. Metz, G. Alici, G.M. Spinks, A finite element model for bending behaviour of conducting polymer electromechanical actuators, Sensor Actuat. A-Phy. 130-131 (2006) 1-11.

20 Z. Uddin, M. Watanabe, H. Shirai, T. Hirai, Effects of plasticizers on novel electromechanical actuations with different poly(vinyl chloride) gels, J. Polym. Sci. B. 41 (2003) 2119-2127.

21 M. Watanabe, T. Kato, M. Suzuki, Y. Hirako, H. Shirai, T. Hirai, Characterization of inhomogeneous polyacrylamide hydrogels, J. Polym. Sci. B. 39 (2001) 1055-1061.

22 F. Carpi, D. De Rossi, R. Kornbluh, R. Pelrine, P.S. Larsen: Dielectric elastomers as electromechanical transducers, Elsevier, Amsterdam, The Netherlands, 2008.

23 H. Gunzler, H.U. Gremlich, IR Spectroscopy, Wiley-VCH.

24 X. Lu, C. Tan, J. Xu, C. He, Thermal degradation of electrical conductivity of polyacrylic acid doped polyaniline: effect of molecular weight of the dopants, Synth. Met. 138 (2003) 429-440.

25 M. Behl, A. Lendlein, Materialstoday, Elsevier, 10 (2007) 20.

26 A. Della Santa, D.D Rossi, A. Mazzoldi, Performance and work capacity of a polppyrrole conducting polymer linear actuator, Synth. Met. 90 (1997) 93-100.

27 M. Shahinpoor, Ionic polymer–conductor composites as biomimetic sensors, robotic actuators and artificial muscles—a review, Electrochimica Acta, 48 (2003) 2343-2353.

28 G. Alici, B. mui, C. Cook, Bending modeling and its experimental verification for conducting polymer actuators dedicated to manipulation applications, Sensor Actuat. A-Phy. 126 (2007) 396-404

29 C.A. Dai, A. Kao, C. Chang, W. Tsai, W. Chen, W. Liu, W. Shih, C.C. Ma, Polymer actuator based on PVA/PAMPS ionic membrane: Optimization of ionic transport properties, Sensor Actuat. A-Phy. 155 (2009) 152-162.

30 J.D. Maddan: Dielectric Elastomers as Electromechanical Transducers, Fundamentals, Materials, Devices, Models and Applications of an Emerging Electroactive Polymer Technology, 2008.

31 S. Yun, J. Kim, C. Song, Performance of Electro-active paper actuators with thickness variation, Sensor Actuat. A-Phy. 133 (2007) 225-230.

32 J. Kim, W. Jung, H. Kim, In-plane strain of electro-active paper under electric fields, Sensor Actuat. A-Phy. 140 (2007) 225-231.

33 A. Mazzoldi, M. Tesconi, A. Tognetti, W. Rocchia, G. Vozzi, G. Pioggia, A. Ahluwalia, D.D. Rossi, Electroactive carbon nanotube actuators: Soft-lithographic fabrication and electro-chemical modelling, Mat. Sci. Eng. C 28 (2008) 1057-1064.

34 T. Yamauchi, S. Tansuriyavong , K. Doi, K. Oshima, M. Shimomura, N. Tsubukawa, J.F.V. Vincent, Preparation of composite materials of polypyrrole and electroactive polymer gel using for actuating system, Synth. Met. 152 (2005) 45-48.

List of table captions

1. Table 1 Electromechanical response of the pure elastomers at T = 300 K

List of figure captions

1. **Figure 1** Experimental setup for the deflection measurement.
2. **Figure 2** Deflection of the elastomers at E = 0 and 600 V/mm: (a) AR70; (b) AR71; (c) AR72; (d) SAR; (e) SIS; (f) SBR; (g) SAR under inversed polarity of electric field; and, (h) SIS under inversed polarity of electric field.

Note: The polarity of the electrode on the right hand side is positive for figures 2(a)–(f) and negative for figures 2(g) and 2(h). The electrode on the left hand side is always GND

3. **Figure 3** (a) Deflection angle of the elastomers vs. electric field strengths; and (b) deflection angle at E = 600 V/mm vs. dielectric constants of the elastomers.
4. **Figure 4** (a) Dielectrophoresis force of the elastomers vs. electric field strength; and (b) dielectrophoresis force at E = 600 V/mm vs. dielectric constants of the elastomers.
5. **Figure 5** Deflection mechanism of elastomers: (a) all specimens without electric field; and (b) acrylic elastomers; (c) SIS; and (d) SAR under applied electric field.

Table 1 Electromechanical response of the pure elastomers at T = 300 K

Type of elastomers	Electrical yield strength (V/mm)	θ (°)	d (mm)	F_d from non-linear deflection theory (mN)	Force density (N/m^3)	Energy density (J/m^3)	Mechanical Power (μW)	Power consumption (mW)	Power density (W/m^3)	Electromechanical coupling efficiency (%)	ε′ (at f = 20 Hz)	Shear modulus at ω =1 rad/s, strain = 1.0% (Pa)
AR70	225	64.7	12.41	0.367	24,732	62,114	0.067	2.66	5.378	0.003	6.21	32,484
AR71	75	70.4	13.29	0.412	28,012	48,910	0.456	5.12	31.01	0.009	6.33	21,604
AR72	75	57.2	11.28	0.318	16,954	15,862	0.179	7.30	9.482	0.002	4.14	10,595
SAR	250	33.4	7.38	0.275	20,446	30,991	0.056	0.80	4.157	0.007	3.95	60,654
SIS	400	11.0	2.44	0.071	3,392	1,428	0.004	1.07	0.102	0.001	2.74	25,777
SBR	375	8.6	1.95	0.157	6,909	785	0.005	0.53	0.220	0.001	2.87	23,397
SAR negative polarity	275	11.7	2.81	0.047	3,253	3,800	0.002	1.44	0.147	0.002	3.95	60,654
SIS negative polarity	375	10.7	2.30	0.118	6,605	1,428	0.003	0.28	0.165	0.001	2.74	25,777

where

d = deflection distance in x axis (mm), l = deflection distance in y axis (mm), θ = deflection angle

τ_i = induction time (sec), τ_r = recovery time (sec)

F_e = elastic force (N) = dEI/l^3 from non-linear deflection theory

F_d = dielectrophoresis force = $mg\sin\theta + F_e$ (N)

Energy density = $\frac{1}{2}E\theta^2$ (J/m^3), Force density = $\frac{F_d}{volume}$ (N/m^3)

Mechanical power = $\frac{1}{4} F_d \frac{d}{\tau_i}$ (μW), τ_i = induction time

Electromechanical coupling efficiency = $\frac{\text{mechanical power}}{\text{power consumption}} \text{x}100\% = \frac{(1/4) * F_d * d}{\text{induction time} * \text{power consumption}} \text{x}100\%$

Power density = $\frac{\text{mechanical power}}{\text{volume}}$ (W/m^3)

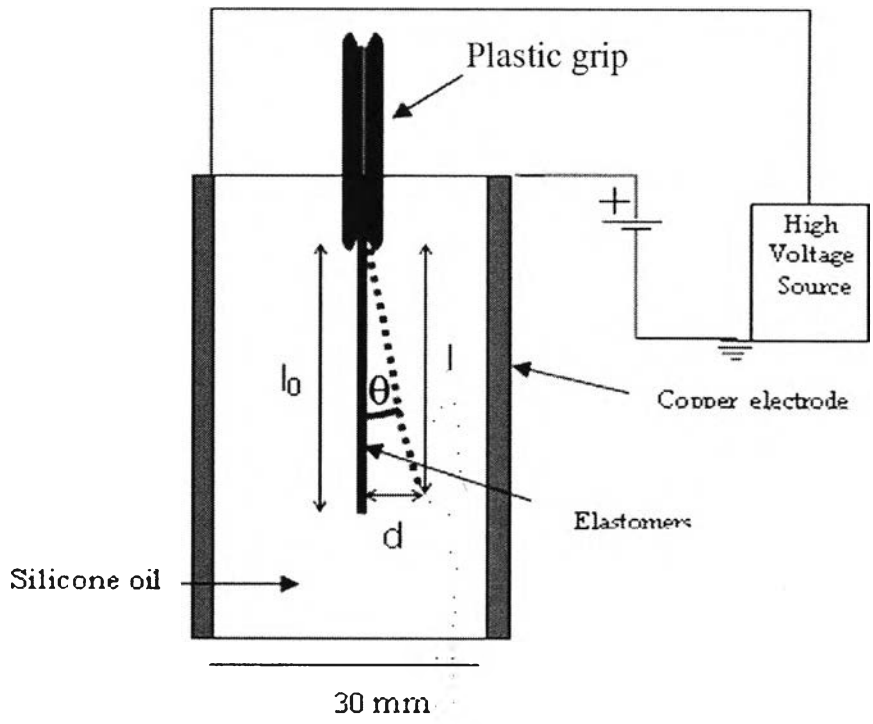

Figure 1 Experimental setup for the deflection measurement.

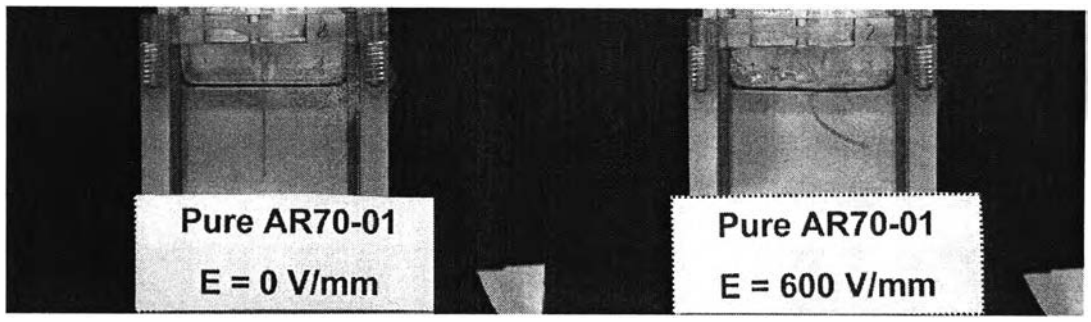
Pure AR70-01
E = 0 V/mm
Pure AR70-01
E = 600 V/mm

(a)

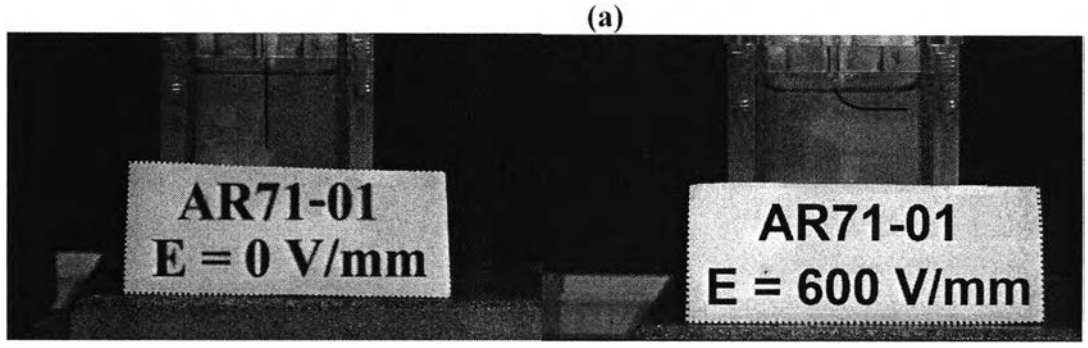
AR71-01
E = 0 V/mm
AR71-01
E = 600 V/mm

(b)

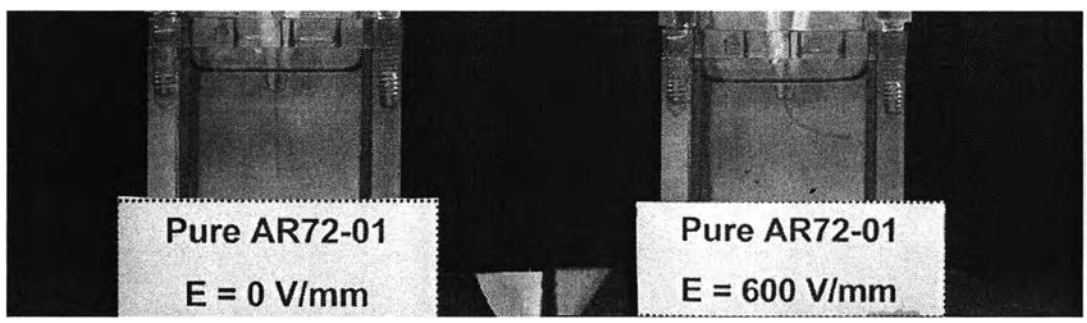
Pure AR72-01
E = 0 V/mm
Pure AR72-01
E = 600 V/mm

(c)

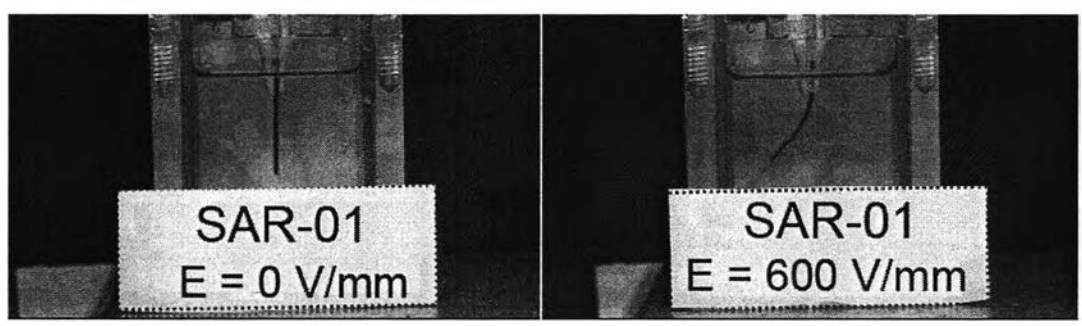
SAR-01
E = 0 V/mm
SAR-01
E = 600 V/mm

(d)

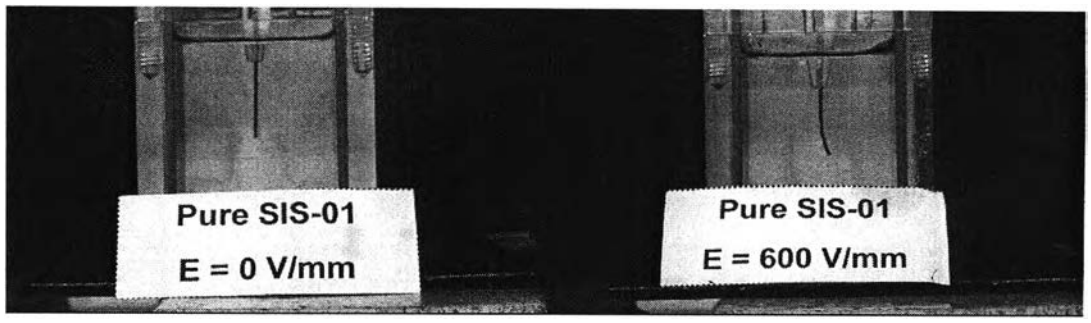

(e)

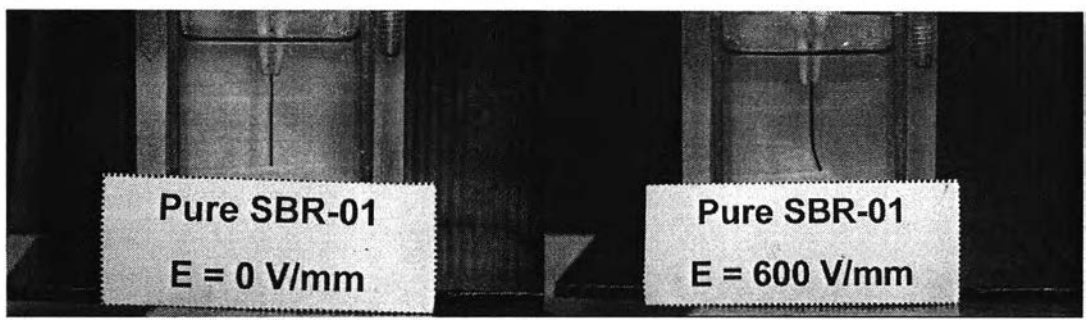

(f)

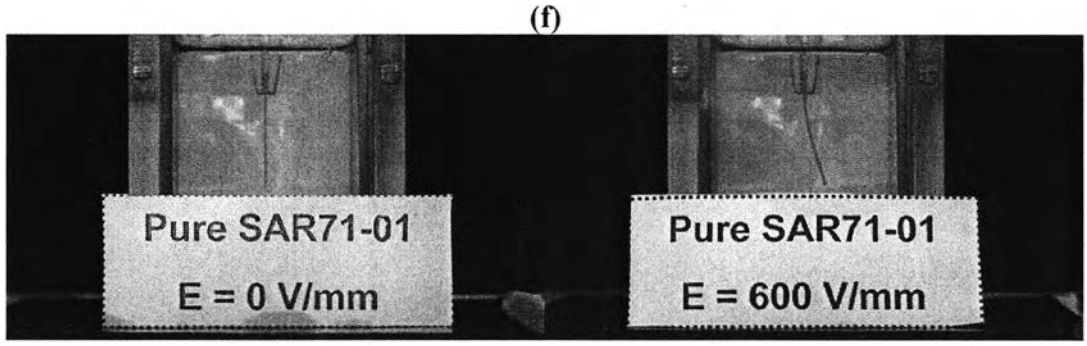

(g)

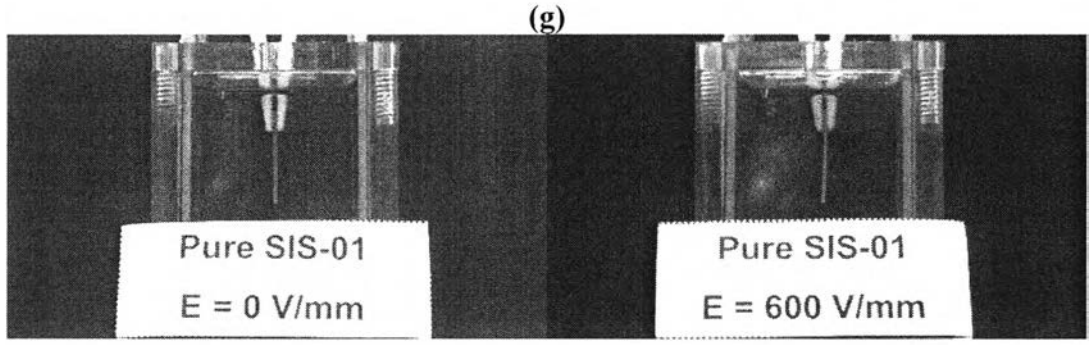

(h)

Figure 2 Deflection of the elastomers at E = 0 and 600 V/mm: (a) AR70; (b) AR71; (c) AR72; (d) SAR; (e) SIS; (f) SBR; (g) SAR under inversed polarity of electric field; and, (h) SIS under inversed polarity of electric field.

Note: The polarity of the electrode on the right hand side is positive for figures 5.2(a)–(f) and negative for figures 5.2(g) and 5.2(h). The electrode on the left hand side is always GND.

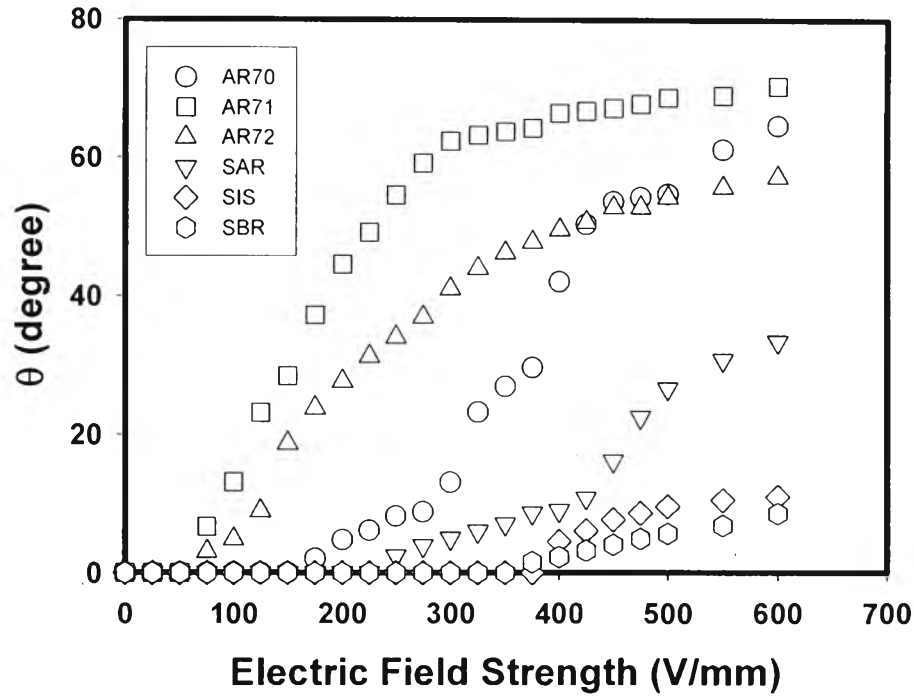

(a)

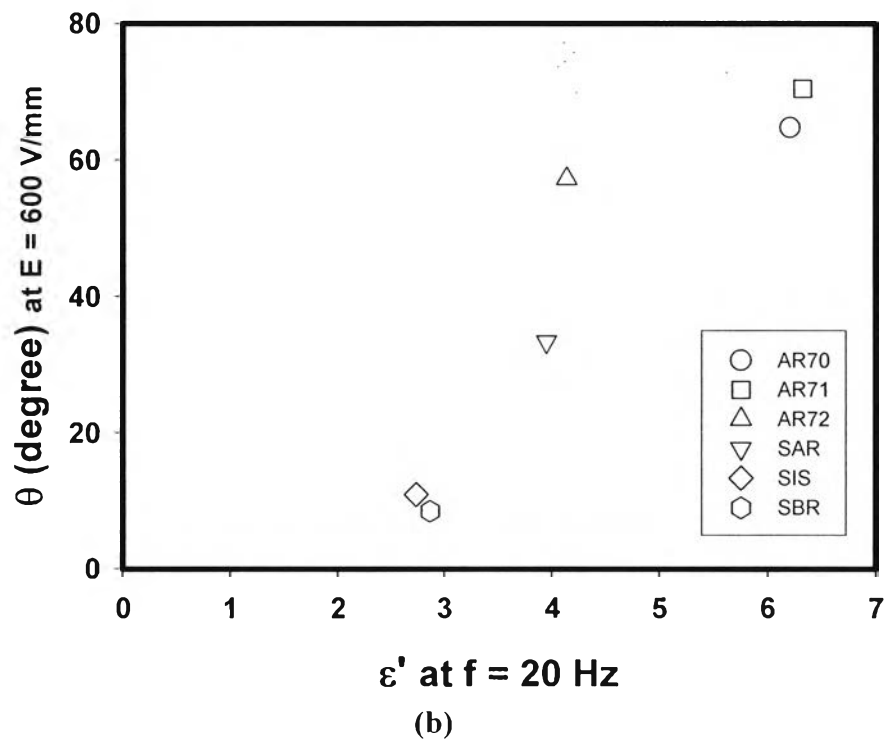

(b)

Figure 3 (a) Deflection angle of the elastomers vs. electric field strengths; and (b) deflection angle at E = 600 V/mm vs. dielectric constants of the elastomers.

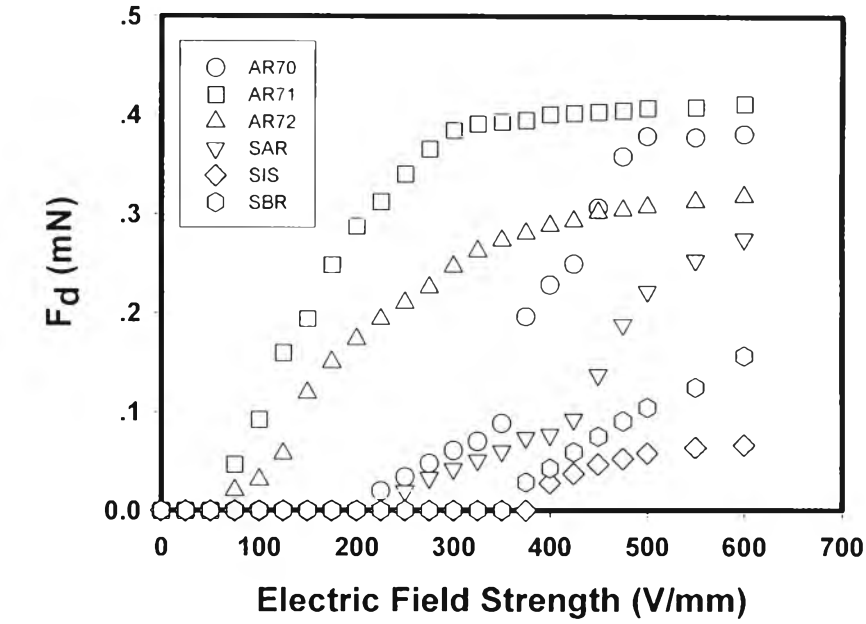

(a)

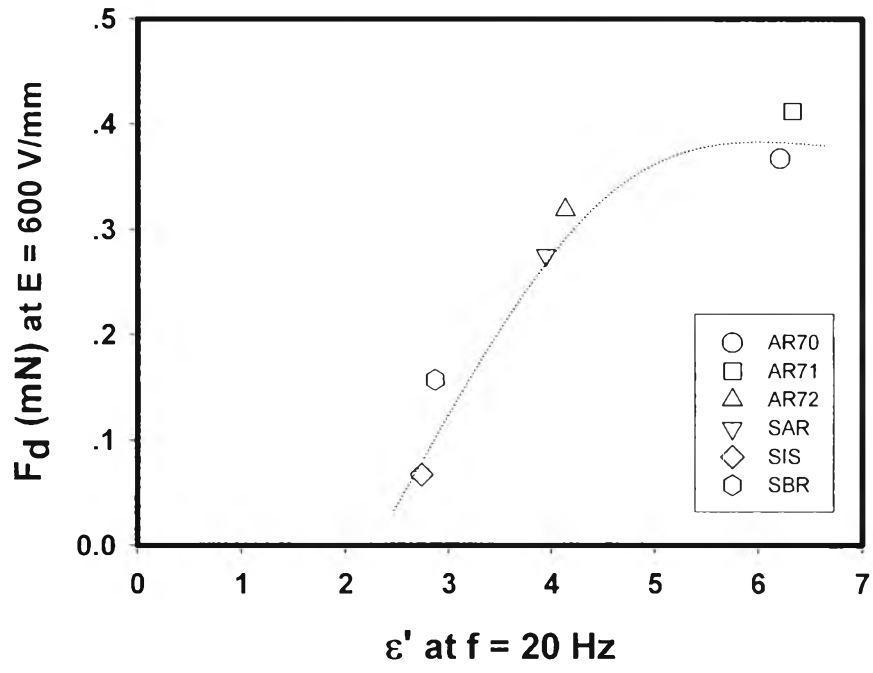

(b)

Figure 4 (a) Dielectrophoresis force of the elastomers vs. electric field strength; and (b) dielectrophoresis force at E = 600 V/mm vs. dielectric constants of the elastomers.

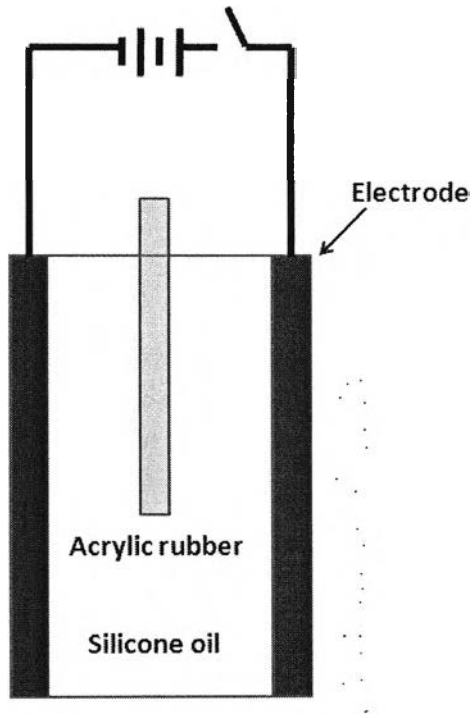
Electrode
Acrylic rubber
Silicone oil

(a)

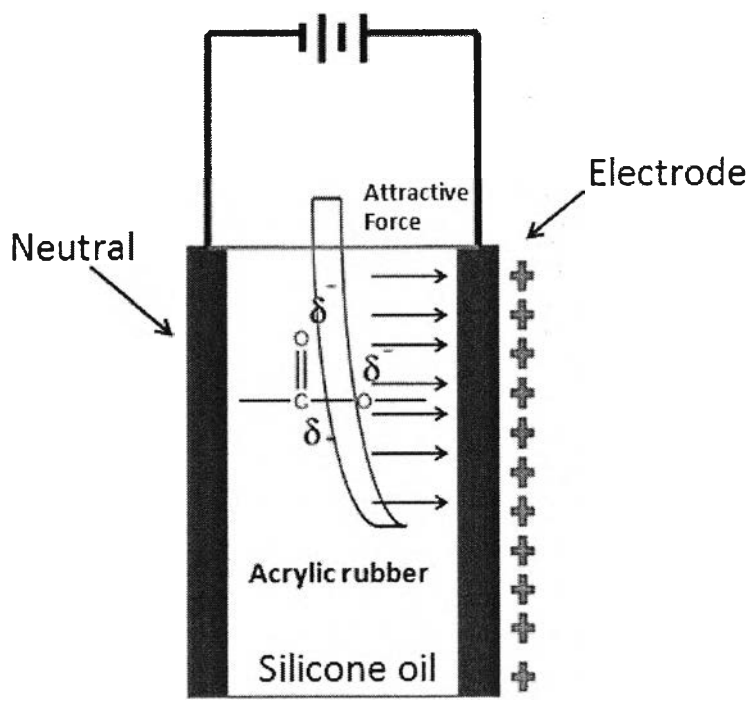
Electrode
Attractive
Force
Neutral
Acrylic rubber
Silicone oil

(b)

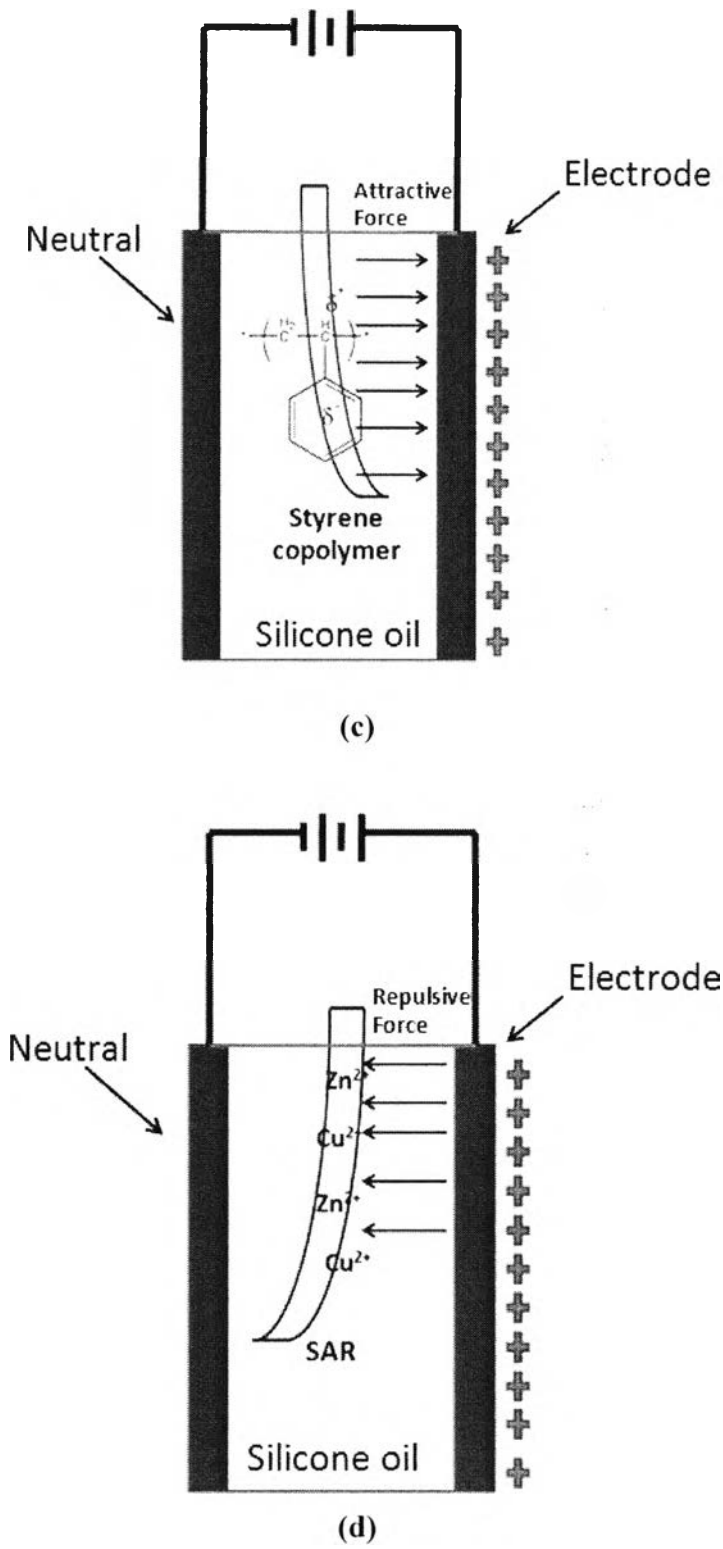

Figure 5 Deflection mechanism of elastomers: (a) specimens without electric field; and (b) acrylic elastomers; (c) SIS; and (d) SAR under applied electric field.